Exotic Photonic Molecules via Lennard-Jones-like Potentials

Przemyslaw Bienias,[1,2] Michael J. Gullans,[1,2,3] Marcin Kalinowski,[1,4] Alexander N. Craddock,[1] Dalia P. Ornelas-Huerta,[1] S. L. Rolston,[1] J. V. Porto,[1] and Alexey V. Gorshkov[1,2]

[1]*Joint Quantum Institute, NIST/University of Maryland, College Park, Maryland 20742, USA*

[2]*Joint Center for Quantum Information and Computer Science, NIST/University of Maryland, College Park, Maryland 20742, USA*

[3]*Department of Physics, Princeton University, Princeton, New Jersey 08544, USA*

[4]*Faculty of Physics, University of Warsaw, Pasteura 5, 02-093 Warsaw, Poland*

(Received 24 March 2020; accepted 5 August 2020; published 26 August 2020)

Ultracold systems offer an unprecedented level of control of interactions between atoms. An important challenge is to achieve a similar level of control of the interactions between photons. Towards this goal, we propose a realization of a novel Lennard-Jones-like potential between photons coupled to the Rydberg states via electromagnetically induced transparency (EIT). This potential is achieved by tuning Rydberg states to a Förster resonance with other Rydberg states. We consider few-body problems in 1D and 2D geometries and show the existence of self-bound clusters ("molecules") of photons. We demonstrate that for a few-body problem, the multibody interactions have a significant impact on the geometry of the molecular ground state. This leads to phenomena without counterparts in conventional systems: For example, three photons in two dimensions preferentially arrange themselves in a line configuration rather than in an equilateral-triangle configuration. Our result opens a new avenue for studies of many-body phenomena with strongly interacting photons.

DOI: 10.1103/PhysRevLett.125.093601

Atomic, molecular, and optical platforms allow for precise control and wide-ranging tunability of system parameters using external fields. Interactions between *atoms* can be controlled via Feshbach resonances enabling studies of the BCS-BEC crossover [1,2] or via highly excited Rydberg states giving rise to frustrated magnetism [3], topological order [4], and other exotic phases [5]. Interactions between single *photons* in vacuum or conventional transparent materials are negligible; however, they can be enhanced by strongly coupling photons to specially engineered matter [6]. An open challenge is to achieve a similar level of tunability for strongly interacting photons as demonstrated for atoms. Such tunability could lead to applications in photonic quantum information processing, metrology, sensing, as well as exotic photonic phases of matter [7].

A promising platform to achieve this goal are Rydberg polaritons, for which interactions between Rydberg states are mapped onto photons via EIT [8–10]. The effective interactions between photons are not only strong [11], but also saturate to a constant value [12–15] for distances shorter than the blockade radius $r_b \sim 10\ \mu$m, which usually is much greater than the wavelength of the photons. These properties have enabled several theoretical proposals and experimental realizations related to quantum information processing, such as gates [16,17], transistors [18–20], and nonclassical states of light [21–24].

Up to now, the field of dispersive Rydberg-EIT has predominantly concentrated on the effective interactions between polaritons proportional to $1/(r_b^6 + r^6)$, which change monotonically as a function of separation r. Additional work has explored lossy [25] Coulomb bound states, and bound states via interactions mediated by 1D photonic crystals [26]. Here, we propose a novel method to tune the shape of the divergence-free interactions [27] in one and two dimensions between photons propagating through the Rydberg medium. We achieve this using Förster resonances, which are a useful tool to control interactions between atoms [9,28–36]. Application of these resonances to quantum optics with Rydberg polaritons was studied in the context of Rydberg atom imaging [37–39] and an all-optical transistor [18,20]. We demonstrate that with an appropriate choice of states and couplings, we can achieve a Lennard-Jones-like potential between photons, which has a global minimum at a finite distance [see Fig. 1(b)]. We show the existence of bound states in one and two dimensions for two photons interacting via this molecular potential, and further discuss multiphoton self-bound clusters (molecules) of photons [see Fig. 1(d)].

In the previous studies of shallow [12] and deep [13] bound states, the photons interacted via a soft-core potential and therefore preferred to overlap. This precluded the formation of more complex molecularlike structures that is possible in our proposal. The many-photon clusters studied here resemble photonic crystalline features studied in one [40,41] and two dimensions [42]. However, the latter proposals are based on strong repulsion and therefore, without the external trapping potential, the crystals become

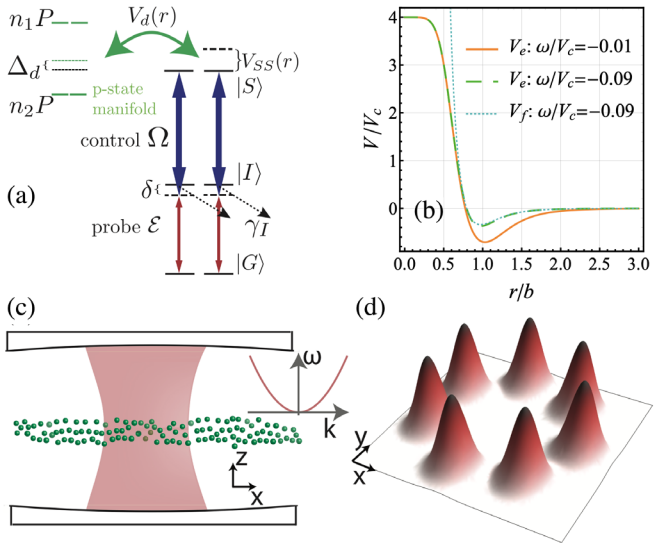

FIG. 1. Using magnetic fields, we tune $|SS\rangle$ (characterized by principal quantum number n) close to the resonance (deviation from resonance denoted by Δ_d) with the P_1P_2 state having $n_1 = n$ and $n_2 = n-1$. (b) This gives rise to the effective molecular potential V_e plotted for $\Delta_d/V_c = 0.03$ used also in Fig. 2(b). By working with $|V_{\min}| \ll 1/|\bar{\chi}|$, this potential around the local minimum is nearly equal to V_f (i.e., is not modified by $\bar{\chi}$), see blue dotted vs green dashed curve. (c) A quasi-2D cloud of atoms placed in the center of a multimode cavity. The mode structure of the cavity gives an effective mass for free particles moving in two dimensions. The inset shows the resulting quadratic photonic dispersion relation. For strong nonlinearities, this setup gives rise to few- and many-body self-bound clusters of light in two dimensions, e.g., arranged on a ring, which is illustrated in (d) for seven photons.

unstable in contrast to our work proposing *self-bound* clusters.

One of the unconventional properties of Rydberg-EIT is strong three- and higher-body interactions between polaritons [43–45]. These strong three-body interactions impact the energies of three-body bound states [46]. Here, we show that Förster resonances in combination with Rydberg-EIT lead to another source of many-body forces. These additional forces give rise to new phenomena. For example, it is energetically favorable to have three polaritons in a line, rather than in a triangular configuration.

System.—Throughout, we focus on photons evolving in 1D and 2D multimode cavities [42,47–50], Fig. 1(c), described by the single-particle Hamiltonian [42,51–55] ($\hbar = 1$)

$$H_1 = \int d\mathbf{r} \begin{pmatrix} \hat{\mathcal{E}} \\ \hat{I} \\ \hat{S} \end{pmatrix}^\dagger \begin{pmatrix} -i\kappa + T & g & 0 \\ g & \Delta & \Omega \\ 0 & \Omega & -i\gamma_S \end{pmatrix} \begin{pmatrix} \hat{\mathcal{E}} \\ \hat{I} \\ \hat{S} \end{pmatrix}, \quad (1)$$

where $\hat{\mathcal{E}}$ is the field operator describing the photonic mode, whereas $\hat{I}$ and $\hat{S}$ describe intermediate- and Rydberg-state collective spin excitations, respectively [8]. 2κ is the cavity loss rate, $\Delta = \delta - i\gamma_I$ is the complex single-photon detuning, $2\gamma_I$ is the atomic intermediate state decay rate, $2\gamma_S$ is the Rydberg level decay rate, g is the single-photon coupling, and Ω is the Rabi frequency of the control drive. The kinetic energy of photons is described in one and two dimensions via $T = -(\nabla^2/2m_{ph})$, where m_{ph} is the photon mass defined by the cavity parameters. Note that our approach can be easily generalized to a 1D free-space geometry, which is discussed below. The Hamiltonian in Eq. (1) can be diagonalized and leads to two bright and one dark polariton branches [13]. Well within the EIT window [56] and in the limit of $\Omega \ll g$ (assumed throughout), the dark-state polariton $\hat{D}$ takes the form $\hat{D} \sim \hat{S} - (\Omega/g)\hat{\mathcal{E}}$. To leading order, the dark-state polariton losses are $(\Omega^2/g^2)\kappa + \gamma_S$ and are negligible for the evolution times considered in this Letter. For simplicity, we shall assume $|\delta| \gg \gamma_I$, and therefore neglect the imaginary part of Δ. The dispersion of $\hat{D}$ is inherited from the photonic component and therefore described via an enhanced mass equal to $m = (g^2/\Omega^2)m_{ph}$.

The interactions for conventional dark-state polaritons are inherited from the van der Waals (vdW) interactions between Rydberg states [10,57] described by the quartic term proportional to $\hat{S}^\dagger(\mathbf{r})\hat{S}^\dagger(\mathbf{r}')V_{SS}(\mathbf{r}-\mathbf{r}')\hat{S}(\mathbf{r}')\hat{S}(\mathbf{r})$. However, close to the Förster resonance, the physics becomes more subtle because at least two strongly interacting pairs of states are involved. To build intuition, we first study the two-body problem.

Effective Lennard-Jones-like potential.—In the past, Förster resonances were used in Rydberg-EIT transistor experiments [18,20], which used two S states with different principal quantum numbers for the gate and source photons. Here, we are interested in few- and many-body physics and therefore use a single nS state [58]. In this case, there is no true Förster resonance at zero external fields [59], but there is an approximate one $nS + nS \to nP + (n-1)P$. We consider $J = 1/2, m_J = 1/2$ S states and $J = 3/2, m_J = 3/2$ P states and tune them to near resonance [20] [see Fig. 1(a)] using a strong magnetic field (defining the quantization axis) perpendicular to the atomic cloud [60].

Under these conditions, there are three relevant pairs of Rydberg states $\{SS, P_1P_2, P_2P_1\}$ with interactions between them described by

$$\begin{pmatrix} V_{SS} & V_d & V_d \\ V_d^* & V_{PP} + \Delta_d & V_{PP,\text{off}} \\ V_d^* & V_{PP,\text{off}} & V_{PP} + \Delta_d \end{pmatrix}, \quad (2)$$

where $\Delta_d = E_{P_1} + E_{P_2} - 2E_S$ is the Förster defect and $V_d = C_3 e^{i2\phi_{12}}/r^3$ is a dipolar interaction with the polar angle ϕ_{12} describing the direction of the relative distance $\mathbf{r} = \mathbf{r}_1 - \mathbf{r}_2$ between the first and second excitation, with $r = |\mathbf{r}|$. In general, $|V_d|$ could have an additional

azimuthal-angle dependence, which is not present for the 1D and 2D geometries considered here. $V_{SS} = C_{SS}/r^6$, $V_{PP} = C_{PP}/r^6$ are diagonal vdW interactions [61], whereas $V_{PP,\mathrm{off}} = C_{PP,\mathrm{off}}/r^6$ is the off-diagonal vdW interaction between P_1P_2 and P_2P_1.

The conventional Rydberg-EIT two-body problem can be described using a set of nine coupled Maxwell-Bloch equations [22,62,63] for XY components of the two-body wave function, where $X, Y \in \{\mathcal{E}, I, S\}$. Importantly, the P_2P_1 and P_1P_2 components are coupled to the conventional equations [22,64] only via dipolar interactions V_d. This enables us to eliminate the P_2P_1 and P_1P_2 components (see Supplemental Material [64]) and leads to the standard equations of motion, but where V_{SS} is replaced by

$$V_f(r) = \frac{C_{SS}}{r^6} - \frac{2(\frac{C_3}{r^3})^2}{\Delta_d + \frac{C_{PP}+C_{PP,\mathrm{off}}}{r^6} - \omega} \tag{3}$$

with ω the total energy of the pair of polaritons. This potential [see Fig. 1(b)] can have a local minimum which intuitively comes from the interplay of the diagonal interactions $\sim 1/r^6$ and the off-diagonal couplings $\sim 1/r^3$: The latter terms dominate at large separation causing the potential curve SS to be attractive, whereas at short distances the vdW interaction dominates and the potential is repulsive. This is in contrast to other molecular potentials [65,66] arising from the avoided crossings between potential curves. Based on V_f, using the approach developed in Ref. [13], we arrive at the soft-core effective potential between polaritons,

$$V_e(r) = \frac{V_f(r)}{1 - \bar{\chi} V_f(r)}, \tag{4}$$

where $\bar{\chi} = (\Delta/2\Omega^2) - (1/2\Delta)$ for the regime considered below. In contrast to conventional Rydberg-EIT, both the strength and shape of V_f can be tuned using Δ_d and the choice of principal quantum numbers. In general, the depth V_{min} of the potential V_e can be as large as its height equal to $-1/\bar{\chi}$. However, by assuming henceforth a shallow V_e such that $V_{\mathrm{min}} \ll \omega_c \equiv 1/|\bar{\chi}|$, we can (i) neglect dependence of $\bar{\chi}$ on ω because $\omega \sim V_{\mathrm{min}}$ [13]; (ii) neglect the scattering to bright polaritons for a small center-of-mass momentum $K \ll k_c \equiv (g^2/c\Omega^2)\omega_c$ [13] assumed henceforth; (iii) neglect blockade-induced three-body interactions [43,44].

Two-body problem.—The two-body problem can be described using the wave function $\varphi(\mathbf{r})$ depending on the relative distance $\mathbf{r}$. φ describes two dark-state polaritons, is proportional to $\mathcal{EE} \sim \mathcal{ES} + \mathcal{SE}$, and is the solution of the effective Schrödinger equation [13]:

$$\omega\varphi(\mathbf{r}) = \left[-\frac{\nabla^2}{m} + V_e(r, \Delta_d, \omega)\right]\varphi(\boldsymbol{r}). \tag{5}$$

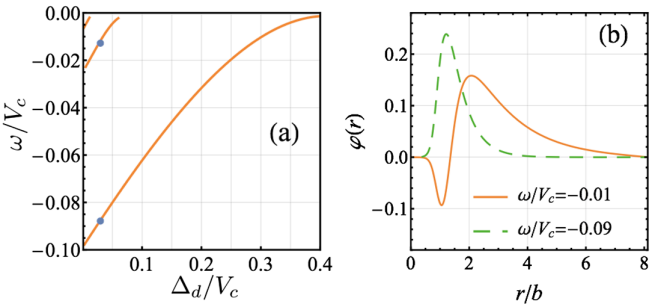

FIG. 2. Results for ^{87}Rb, $n = 120$, $n_1 = 120$, $n_2 = 119$, $\Omega < |\Delta|$, $V_c m b^2 = 40$, and $\omega_c = 4V_c$, which is achieved by an appropriate choice of Ω. (a) Bound-state energies as a function of Δ_d in units of V_c. (b) The wave functions for two lowest bound states with $\Delta_d/V_c = 0.03$ [blue dots in (a)].

As discussed, we can neglect dependence of $\bar{\chi}$ on ω, however, there is still dependence of V_f on ω, see Eq. (3), which we take into account in the numerics. The local minimum of V_e exists for $C_{SS}(\omega - \Delta_d) + 2C_3^2 > 0$. Considering $|\omega| \ll \Delta_d$ enables us to define the characteristic energy $\nu_c = 2C_3^2/C_{SS}$ quantifying the range of Δ_d for which a bound state could exist. In addition, we define (for details see the Supplemental Material [64]) the characteristic length scale $b = [(\sqrt{2}+1)C_{PP}C_{SS}/C_3^2]^{1/6}$ for the position of the local minimum, and $V_c = 2C_3^2/C_{PP}$ quantifying the depth of the potential.

Next, we self-consistently find the solutions of Eq. (5) for different Δ_d. In Fig. 2, we show solutions for the 1D limit of Eq. (5) for $V_c m b^2 = 40$, corresponding to $\mathrm{OD}_b \gamma_I/\delta = 0.9$, where $\mathrm{OD}_b \equiv \mathrm{OD}(b/L)$ is an optical depth OD per b. The smaller the ratio Δ_d/V_c is, the deeper V_f is and, therefore, the second (and even third) bound state can be seen in Fig. 2(a). The lowest bound state [green in Fig. 2(b)] has a width smaller than the first excited bound state (orange), the latter having a single node around the local minimum of V_e at $r \approx b$, Fig. 1(b). Both wave functions are strongly suppressed at short distances due to the strong repulsion for small r.

Three and more photons.—For conventional few-body problems, it is usually a good approximation to assume that each pair of bodies interacts via a two-body potential. However, Rydberg polaritons are an unconventional platform enabling strong many-body interactions, as was shown for a soft-core potential V_e in Refs. [43,44,46]. In this Letter, we can neglect these higher-body interactions because states of interest are largely supported outside the repulsive core of the potential, and therefore, the three-body forces are strongly suppressed for $|\bar{\chi} V_{\mathrm{min}}| \ll 1$, Refs. [43–45]. However, we show that Förster resonances in combination with Rydberg-EIT lead to another source of many-body forces.

Even though the SS channel is on resonance with two channels P_1P_2 and P_2P_1, the majority of the three-body

physics can be well-described by a single effective channel $PP \sim P_1P_2 + P_2P_1$ [64] (note that all the numerics are performed without this approximation). The dipolar interaction between states $\{SSS, SPP, PSP, PPS\}$ takes the form

$$\begin{pmatrix} V_S & V_{d,23} & V_{d,13} & V_{d,12} \\ V_{d,23}^* & V_{P,1}+\Delta_d & W_{12} & W_{13} \\ V_{d,13}^* & W_{12} & V_{P,2}+\Delta_d & W_{23} \\ V_{d,12}^* & W_{13} & W_{23} & V_{P,3}+\Delta_d \end{pmatrix}, \quad (6)$$

where $V_{P,i} = V_{PP}(r_j - r_k) + V_{SP}(r_i - r_j) + V_{SP}(r_i - r_k)$ with $i \neq j$, k and $j < k$ describes all vdW interactions between involved Rydbergs; V_S is a sum of vdW interactions between all polaritons in S state. $V_{d,ij} = \sqrt{2}C_3 e^{i2\phi_{ij}}/|\mathbf{r}_i - \mathbf{r}_j|^3$ is the effective dipole interaction between SS and PP. Analogously, $W_{ij}(r) = -\frac{1}{2}C_3/|\mathbf{r}_i - \mathbf{r}_j|^3$ describes the dipole interaction between SP and PS. Without off-diagonal W terms, we could eliminate all components containing P states. However, due to these exchange terms, this is no longer possible, which is one of the reasons for the strong N body forces.

Low-energy regime.—The low energy assumption, $T_i \ll |V_{\min}|$ (where T_i is the kinetic energy of the ith polariton), together with the already made assumption that $|V_{\min}| \ll \omega_c$, ensures that the dipolar interactions modify the internal composition of the dark states only weakly [40]. Therefore, we can neglect the blockade effects on the effective interaction V_e and dark-state polaritons. In the slow-light regime of $g \gg \Omega$, dark states D have a negligible contribution from $\mathcal{E}$ and I and mostly consist of Rydberg states. Hence, the dipolar Hamiltonian Eq. (6) maps directly onto dark-state polaritons D and collective excitations P. That is, the full Hamiltonian describing the evolution of the three polaritons in the $\{DDD, DPP, PDP, PPD\}$ basis is a sum of Eq. (6) with kinetic terms $\{T_1 + T_2 + T_3, T_1, T_2, T_3\}$ on the diagonals.

Few-body bound states in the large-mass limit.—To give additional insights into the role of few-body interactions in the many-body problem, in the following we neglect kinetic energy all together. This requires $V_c \gg 1/mb^2$ and therefore $\mathrm{OD}_b \gg (\delta/\gamma_I)$. Next, we numerically solve for the eigenstates of the two-channel version [64] of the Hamiltonian Eq. (6) as a function of separations r_{ij} in a 2D geometry. We find that it is preferable to have three polaritons in a line rather than in an equilateral-triangle configuration. Moreover, the configuration in which one photon is away from the dimer has lower energy than the equilateral-triangle configuration. This is demonstrated in Figs. 3(a)–3(b) where (a) shows total energies for the polaritons being at the corners of an isosceles triangle and (b) shows that regardless of the value of Δ_d/ν_c, the line configuration has the lowest energy [67].

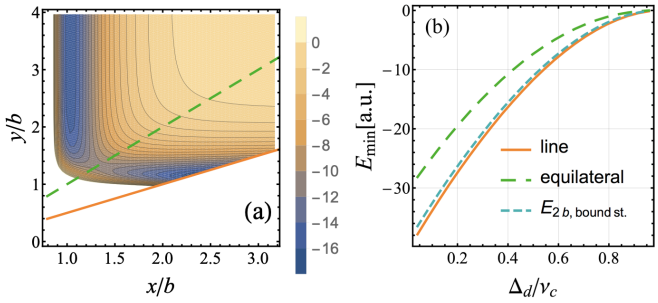

FIG. 3. Self-consistent solution of Eq. (6) describing polaritons in the large-mass limit. (a) Three-body problem in the isosceles triangular configuration with edge lengths y, y, x. (b) Lowest energy as a function of Δ_d for line, regular-polygon, and dimer configurations for three bodies. Results are for ^{87}Rb with n_1, n_2, n as in Fig. 2. Additionally, (a) is for $\Delta_d/\nu_c = 0.4$.

Intuition behind the N-body force.—For the three-body problem, even approximate analytical expressions for eigenstates of Eq. (6) are lengthy for arbitrary separations. Therefore, we use an equilateral-triangle configuration parametrized by edge length r to obtain more intuition on the three-body forces. The energy E being the lowest eigenvalue of Eq. (6) as a function of the separation r, for $E \ll \Delta_d$, takes the form

$$E = 3\left(\frac{C_{SS}}{r^6} - \frac{2(\frac{C_3}{r^3})^2}{\Delta_d + \frac{C_{PP}+2C_{SP}}{r^6} - W(r)}\right). \quad (7)$$

From comparison of this expression with Eq. (3), we see that the denominator has two additional terms [68]: (i) the vdW energy shift $2C_{SP}/r^6$, and (ii) the shift due to the off-diagonal dipolar interactions $W(r) < 0$ [69]. Both lead to the suppression of E, resulting in strong three-body repulsion which prevents configurations with three particles closely spaced. This gives rise to the novel ground state geometries presented in Fig. 3.

Multiple-body problem.—From Fig. 4(a), we see that the few-body forces lead to an effect in which many photons prefer to be arranged as independent dimers. For Cs [see Fig. 4(b)] at large enough N (which depends on Δ_d/ν_q, and for $\Delta_d/\nu_q = 0.4$ happens for $N \geq 7$), a regular polygon (ring) is the ground state rather than a linear configuration [see Fig. 1(d)]. Intuitively, the additional two-body attractive bond for the ring arrangement wins over the additional repulsive many-body forces present in this configuration.

Experimental realization.—Photons in a multimode cavity [42] enable us to tune the polariton's mass so that mV_e is repulsive at short distances, has local minima at finite distance, and is free of potentially lossy divergences [13,27,70]. In general, for multimode cavities, the generation of the mass is intertwined with the presence of the trapping potential. However, for a near-planar cavity (defined as $R \gg L$, where R is mirror curvature and L distance between mirrors) we have $m_{ph} = (k/c)$ and the

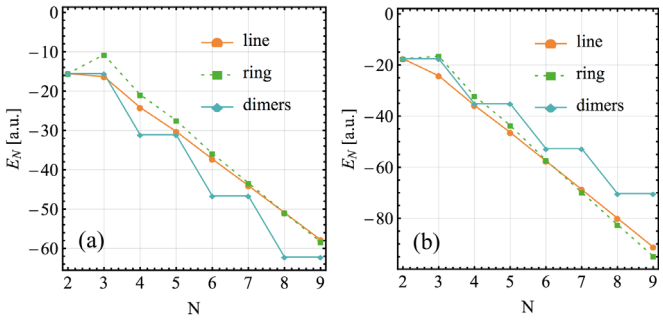

FIG. 4. The lowest energy for on-the-line and on-the-ring configurations for $\Delta_d/\nu_c = 0.4$ for (a) Rb and (b) Cs. We see that strong N-body forces lead to different geometry of the ground state depending on N and the atomic species.

trapping frequency $\omega_{\mathrm{tr}} = (c/\sqrt{2LR})$. Therefore, the trapping vanishes with increasing LR.

Note that our scheme also works in a free-space quasi-1D geometry [22] for a magnetic field perpendicular to the propagation direction and the transverse mass much greater than the longitudinal one [70]. Then, by working in the regime $\Omega > |\Delta|$, we can achieve a divergence-free potential that is repulsive at short distances [13,27].

To prepare the ground state on small systems we envision a spectroscopic post-selection approach whereby a weak product coherent state wave function is input with the mode frequencies chosen to add up to the energy of the target ground state. The mode functions of the photons can be further chosen to maximize the ground-state overlap. State preparation is then possible through postselection on the total photon number. The weak input condition ensures that the target manifold is not spoiled by dissipation from higher-photon number manifolds. For larger systems, more efficient preparation schemes become necessary that are still insensitive to dissipation. We imagine using dissipative Rydberg blockade [21,22] to prepare a product state of many single photons as the starting state for adiabatic transfer to the ground state. This method is robust to dissipation for ground state gaps larger than the dissipation rate. Once the state is prepared, the measured multibody 2D correlation functions can be postprocessed [71] to prevent the rotational symmetry and shot-to-shot variations in measurement outcomes from smearing out spatial patterns. We leave a more complete and detailed analysis of preparation and detection for future work.

Outlook.—In this work, we concentrated on the strongly interacting regime in one and two dimensions. Another direction is a study of the 3D interacting regime of photons copropagating in free space in the presence of the molecular potential in the transverse directions [70,72]. Note that our analysis suggests that the strong few-body forces can also be observed in experiments with ultracold Rydberg atoms alone [73,74] rather than Rydberg polaritons. This can be done in a 2D pancake geometry with or without an additional optical lattice potential. It is an especially promising direction in the light of recent work on the observation of Rydberg macrodimers [65] with P states close to Förster resonances.

We thank H. P. Buechler, S. Hofferberth, I. Lesanovsky, J. Young, Y. Wang, and S. Weber for insightful discussion. P. B., M. K., A. C, D. O.-H, S. L. R., J. V. P., and A. V. G. acknowledge support from the United States Army Research Lab's Center for Distributed Quantum Information (CDQI) at the University of Maryland and the Army Research Lab, and support from the National Science Foundation Physics Frontier Center at the Joint Quantum Institute (Grant No. PHY1430094). P. B., M. K., and A. V. G. additionally acknowledge support from AFOSR, ARO MURI, DOE ASCR Quantum Testbed Pathfinder program (Award No. DE-SC0019040), DOE BES Materials and Chemical Sciences Research for Quantum Information Science program (Award No. DE-SC0019449), DOE ASCR Accelerated Research in Quantum Computing program (Award No. DE-SC0020312), and NSF PFCQC program. M. K. acknowledges financial support from the Foundation for Polish Science within the First Team program co-financed by the European Union under the European Regional Development Fund.

[1] I. Bloch, W. Zwerger, and J. Dalibard, Many-body physics with ultracold gases, Rev. Mod. Phys. **80**, 885 (2008).
[2] C. Chin, R. Grimm, P. Julienne, and E. Tiesinga, Feshbach resonances in ultracold gases, Rev. Mod. Phys. **82**, 1225 (2010).
[3] R. M. W. van Bijnen and T. Pohl, Quantum Magnetism and Topological Ordering via Rydberg Dressing near Förster Resonances, Phys. Rev. Lett. **114**, 243002 (2015).
[4] A. W. Glaetzle, M. Dalmonte, R. Nath, C. Gross, I. Bloch, and P. Zoller, Designing Frustrated Quantum Magnets with Laser-Dressed Rydberg Atoms, Phys. Rev. Lett. **114**, 173002 (2015).
[5] T. Grass, P. Bienias, M. J. Gullans, R. Lundgren, J. Maciejko, and A. V. Gorshkov, Fractional Quantum Hall Phases of Bosons with Tunable Interactions: From the Laughlin Liquid to a Fractional Wigner Crystal, Phys. Rev. Lett. **121**, 253403 (2018).
[6] D. E. Chang, V. Vuletić, and M. D. Lukin, Quantum nonlinear optics: Photon by photon, Nat. Photonics, **8**, 685 (2014).
[7] T. Caneva, M. T. Manzoni, T. Shi, J. S. Douglas, J. I. Cirac, and D. E. Chang, Quantum dynamics of propagating photons with strong interactions: A generalized input-output formalism, New J. Phys. **17**, 113001 (2015).
[8] M. Fleischhauer and M. D. Lukin, Dark-State Polaritons in Electromagnetically Induced Transparency, Phys. Rev. Lett. **84**, 5094 (2000).
[9] M. D. Lukin, M. Fleischhauer, R. Cote, L. M. Duan, D. Jaksch, J. I. Cirac, and P. Zoller, Dipole Blockade and Quantum Information Processing in Mesoscopic Atomic Ensembles, Phys. Rev. Lett. **87**, 037901 (2001).

[10] I. Friedler, D. Petrosyan, M. Fleischhauer, and G. Kurizki, Long-range interactions and entanglement of slow single-photon pulses, Phys. Rev. A **72**, 043803 (2005).
[11] J. D. Pritchard, D. Maxwell, A. Gauguet, K. J. Weatherill, M. P. A. Jones, and C. S. Adams, Cooperative Atom-Light Interaction in a Blockaded Rydberg Ensemble, Phys. Rev. Lett. **105**, 193603 (2010).
[12] O. Firstenberg, T. Peyronel, Q. Y. Liang, A. V. Gorshkov, M. D. Lukin, and V. Vuletić, Attractive photons in a quantum nonlinear medium, Nature (London) **502**, 71 (2013).
[13] P. Bienias, S. Choi, O. Firstenberg, M. F. Maghrebi, M. Gullans, M. D. Lukin, A. V. Gorshkov, and H. P. Büchler, Scattering resonances and bound states for strongly interacting Rydberg polaritons, Phys. Rev. A **90**, 053804 (2014).
[14] P. Bienias, Few-body quantum physics with strongly interacting Rydberg polaritons, Eur. Phys. J. Spec. Top. **225**, 2957 (2016).
[15] P. Bienias and H. P. Büchler, Two photon conditional phase gate based on Rydberg slow light polaritons, J. Phys. B **53**, 054003 (2020).
[16] D. Tiarks, S. Schmidt-Eberle, T. Stolz, G. Rempe, and S. Dürr, A photon–photon quantum gate based on Rydberg interactions, Nat. Phys. **15**, 124 (2019).
[17] D. Tiarks, S. Schmidt, G. Rempe, and S. Dürr, Optical π phase shift created with a single-photon pulse, Sci. Adv. **2**, e1600036 (2016).
[18] D. Tiarks, S. Baur, K. Schneider, S. Dürr, and G. Rempe, Single-Photon Transistor Using a Förster Resonance, Phys. Rev. Lett. **113**, 053602 (2014).
[19] H. Gorniaczyk, C. Tresp, J. Schmidt, H. Fedder, and S. Hofferberth, Single-Photon Transistor Mediated by Interstate Rydberg Interactions, Phys. Rev. Lett. **113**, 053601 (2014).
[20] H. Gorniaczyk, C. Tresp, P. Bienias, A. Paris-Mandoki, W. Li, I. Mirgorodskiy, H. P. Büchler, I. Lesanovsky, and S. Hofferberth, Enhancement of Rydberg-mediated single-photon nonlinearities by electrically tuned Förster resonances, Nat. Commun. **7**, 12480 (2016).
[21] Y. O. Dudin and A. Kuzmich, Strongly interacting Rydberg excitations of a cold atomic gas, Science **336**, 887 (2012).
[22] T. Peyronel, O. Firstenberg, Q. Y. Liang, S. Hofferberth, A. V. Gorshkov, T. Pohl, M. D. Lukin, and V. Vuletić, Quantum nonlinear optics with single photons enabled by strongly interacting atoms, Nature (London) **488**, 57 (2012).
[23] D. O. Huerta, A. Craddock, E. Goldschmidt, A. Hachtel, Y. Wang, P. Bienias, A. Gorshkov, S. Rolston, and J. Porto, On-demand indistinguishable single photons from an efficient and pure source based on a Rydberg ensemble, Optica **7**, 813 (2020).
[24] P. Bienias, J. Douglas, A. Paris-Mandoki, P. Titum, I. Mirgorodskiy, C. Tresp, E. Zeuthen, M. J. Gullans, M. Manzoni, S. Hofferberth, D. Chang, and A. V. Gorshkov, Photon propagation through dissipative Rydberg media at large input rates, Phys. Rev. Research **2**, 033049 (2020).
[25] These bound states [27] are based on the singular potentials that lead to significant losses for experimentally relevant parameters.
[26] J. S. Douglas, T. Caneva, and D. E. Chang, Photon Molecules in Atomic Gases Trapped near Photonic Crystal Waveguides, Phys. Rev. X **6**, 031017 (2016).
[27] M. F. Maghrebi, M. J. Gullans, P. Bienias, S. Choi, I. Martin, O. Firstenberg, M. D. Lukin, H. P. Büchler, and A. V. Gorshkov, Coulomb Bound States of Strongly Interacting Photons, Phys. Rev. Lett. **115**, 123601 (2015).
[28] K. Afrousheh, P. Bohlouli-Zanjani, D. Vagale, A. Mugford, M. Fedorov, and J. D. Martin, Spectroscopic Observation of Resonant Electric Dipole-Dipole Interactions between Cold Rydberg Atoms, Phys. Rev. Lett. **93**, 233001 (2004).
[29] P. Bohlouli-Zanjani, J. A. Petrus, and J. D. Martin, Enhancement of Rydberg Atom Interactions Using ac Stark Shifts, Phys. Rev. Lett. **98**, 203005 (2007).
[30] T. Vogt, M. Viteau, J. Zhao, A. Chotia, D. Comparat, and P. Pillet, Dipole Blockade at Förster Resonances in High Resolution Laser Excitation of Rydberg States of Cesium Atoms, Phys. Rev. Lett. **97**, 083003 (2006).
[31] I. I. Ryabtsev, D. B. Tretyakov, I. I. Beterov, and V. M. Entin, Observation of the Stark-Tuned Förster Resonance between Two Rydberg Atoms, Phys. Rev. Lett. **104**, 073003 (2010).
[32] A. Reinhard, K. C. Younge, T. C. Liebisch, B. Knuffman, P. R. Berman, and G. Raithel, Double-Resonance Spectroscopy of Interacting Rydberg-Atom Systems, Phys. Rev. Lett. **100**, 233201 (2008).
[33] J. Nipper, J. B. Balewski, A. T. Krupp, S. Hofferberth, R. Löw, and T. Pfau, Atomic Pair-State Interferometer: Controlling and Measuring an Interaction-Induced Phase Shift in Rydberg-Atom Pairs, Phys. Rev. X **2**, 031011 (2012).
[34] S. Ravets, H. Labuhn, D. Barredo, T. Lahaye, and A. Browaeys, Measurement of the angular dependence of the dipole-dipole interaction between two individual Rydberg atoms at a Förster resonance, Phys. Rev. A **92**, 020701(R) (2015).
[35] B. Pelle, R. Faoro, J. Billy, E. Arimondo, P. Pillet, and P. Cheinet, Quasiforbidden two-body Förster resonances in a cold Cs Rydberg gas, Phys. Rev. A **93**, 023417 (2016).
[36] I. I. Beterov and M. Saffman, Rydberg blockade, Förster resonances, and quantum state measurements with different atomic species, Phys. Rev. A **92**, 042710 (2015).
[37] G. Günter, M. Robert-de Saint-Vincent, H. Schempp, C. S. Hofmann, S. Whitlock, and M. Weidemüller, Interaction Enhanced Imaging of Individual Rydberg Atoms in Dense Gases, Phys. Rev. Lett. **108**, 013002 (2012).
[38] B. Olmos, W. Li, S. Hofferberth, and I. Lesanovsky, Amplifying single impurities immersed in a gas of ultracold atoms, Phys. Rev. A **84**, 041607(R) (2011).
[39] G. Guenter, H. Schempp, M. Robert-de Saint-Vincent, V. Gavryusev, S. Helmrich, C. S. Hofmann, S. Whitlock, and M. Weidemueller, Observing the dynamics of dipole-mediated energy transport by interaction-enhanced imaging, Science **342**, 954 (2013).
[40] J. Otterbach, M. Moos, D. Muth, and M. Fleischhauer, Wigner Crystallization of Single Photons in Cold Rydberg Ensembles, Phys. Rev. Lett. **111**, 113001 (2013).
[41] D. E. Chang, V. Gritsev, G. Morigi, V. Vuletić, M. D. Lukin, and E. A. Demler, Crystallization of strongly interacting photons in a nonlinear optical fibre, Nat. Phys. **4**, 884 (2008).
[42] A. Sommer, H. P. Büchler, and J. Simon, Quantum crystals and Laughlin droplets of cavity Rydberg polaritons, arXiv:1506.00341.

[43] K. Jachymski, P. Bienias, and H. P. Büchler, Three-Body Interactions of Slow Light Rydberg Polaritons, Phys. Rev. Lett. **117**, 053601 (2016).
[44] M. J. Gullans, J. D. Thompson, Y. Wang, Q. Y. Liang, V. Vuletić, M. D. Lukin, and A. V. Gorshkov, Effective Field Theory for Rydberg Polaritons, Phys. Rev. Lett. **117**, 113601 (2016).
[45] M. Kalinowski, Y. Wang, P. Bienias, M. J. Gullans, D. Ornelas-Huerta, A. N. Craddock, S. Rolston, H. P. Buechler, and A. V. Gorshkov, Enhancement and tunability of three-body loss between strongly interacting photons (in preparation).
[46] Q.-Y. Liang, A. V. Venkatramani, S. H. Cantu, T. L. Nicholson, M. J. Gullans, A. V. Gorshkov, J. D. Thompson, C. Chin, M. D. Lukin, and V. Vuletić, Observation of three-photon bound states in a quantum nonlinear medium, Science **359**, 783 (2018).
[47] A. Sommer and J. Simon, Engineering photonic Floquet Hamiltonians through Fabry-Pérot resonators, New J. Phys. **18**, 035008 (2016).
[48] N. Schine, A. Ryou, A. Gromov, A. Sommer, and J. Simon, Synthetic Landau levels for photons, Nature (London) **534**, 671 (2016).
[49] N. Jia, N. Schine, A. Georgakopoulos, A. Ryou, L. W. Clark, A. Sommer, and J. Simon, A strongly interacting polaritonic quantum dot, Nat. Phys. **14**, 550 (2018).
[50] L. W. Clark, N. Jia, N. Schine, C. Baum, A. Georgakopoulos, and J. Simon, Interacting Floquet polaritons, Nature (London) **532**, 571 (2019).
[51] V. Parigi, E. Bimbard, J. Stanojevic, A. J. Hilliard, F. Nogrette, R. Tualle-Brouri, A. Ourjoumtsev, and P. Grangier, Observation and Measurement of "Giant" Dispersive Optical Nonlinearities in an Ensemble of Cold Rydberg Atoms, Phys. Rev. Lett. **109**, 233602 (2012).
[52] J. Stanojevic, V. Parigi, E. Bimbard, A. Ourjoumtsev, and P. Grangier, Dispersive optical nonlinearities in a Rydberg electromagnetically-induced-transparency medium, Phys. Rev. A **88**, 053845 (2013).
[53] A. Georgakopoulos, A. Sommer, and J. Simon, Theory of interacting cavity Rydberg polaritons, Quantum Sci. Technol. **4**, 014005 (2018).
[54] E. T. Marina Litinskaya and G. Pupillo, Cavity polaritons with Rydberg blockade and long-range interactions, J. Phys. B **49**, 164006 (2016).
[55] A. Grankin, E. Brion, E. Bimbard, R. Boddeda, I. Usmani, A. Ourjoumtsev, and P. Grangier, Quantum statistics of light transmitted through an intracavity Rydberg medium, New J. Phys. **16**, 043020 (2014).
[56] D. Petrosyan, J. Otterbach, and M. Fleischhauer, Electromagnetically Induced Transparency with Rydberg Atoms, Phys. Rev. Lett. **107**, 213601 (2011).
[57] A. K. Mohapatra, M. G. Bason, B. Butscher, K. J. Weatherill, and C. S. Adams, A giant electro-optic effect using polarizable dark states, Nat. Phys. **4**, 890 (2008).
[58] One could imagine studying a two-component dark-state polariton (DSP) system, where for each Rydberg S state the DSP exists. This, however, is experimentally more challenging (requiring more lasers), as well as theoretically more complicated, and lacking the simplicity of the single-component approach we discuss here.
[59] T. G. Walker and M. Saffman, Consequences of Zeeman degeneracy for the van der Waals blockade between Rydberg atoms, Phys. Rev. A **77**, 032723 (2008).
[60] For the other choice of m_J for the P state, the selection rules would have to be modified because for the considered magnetic fields we are entering the Paschen-Back regime.
[61] They are computed by excluding the channels that are taken into account explicitly in Eq. (2).
[62] A. V. Gorshkov, J. Otterbach, M. Fleischhauer, T. Pohl, and M. D. Lukin, Photon-Photon Interactions via Rydberg Blockade, Phys. Rev. Lett. **107**, 133602 (2011).
[63] P. Bienias and H. P. Büchler, Quantum theory of Kerr nonlinearity with Rydberg slow light polaritons, New J. Phys. **18**, 123026 (2016).
[64] See Supplemental Material at http://link.aps.org/supplemental/10.1103/PhysRevLett.125.093601 for the detailed derivation of the V_f, the details on the characteristic units in the problem, the relation between the PP channel and P_1P_2, P_2P_1 channels, and a self-consistent solution of the four body problem.
[65] S. Hollerith, J. Zeiher, J. Rui, A. Rubio-Abadal, V. Walther, T. Pohl, D. M. Stamper-Kurn, I. Bloch, and C. Gross, Quantum gas microscopy of Rydberg macrodimers, Science 2019) 664 ,**364**).
[66] D. Petrosyan and K. Mølmer, Binding Potentials and Interaction Gates between Microwave-Dressed rydberg Atoms, Phys. Rev. Lett. **113**, 123003 (2014).
[67] We numerically confirmed that neither the triangular nor the dimer configuration is a metastable state.
[68] Note that $C_{PP} + C_{PP,\mathrm{off}}$ in Eq. (3) corresponds to C_{PP} in the equation above.
[69] $W(r)$ is < 0 because transition dipole elements for the considered levels satisfy $\langle SP_j|\hat{d}^-\hat{d}^+|P_jS\rangle < 0$.
[70] M. J. Gullans, S. Diehl, S. T. Rittenhouse, B. P. Ruzic, J. P. D'Incao, P. Julienne, A. V. Gorshkov, and J. M. Taylor, Efimov States of Strongly Interacting Photons, Phys. Rev. Lett. **119**, 233601 (2017).
[71] P. Schauss, M. Cheneau, M. Endres, T. Fukuhara, S. Hild, A. Omran, T. Pohl, C. Gross, S. Kuhr, and I. Bloch, Observation of spatially ordered structures in a two-dimensional Rydberg gas, Nature (London) **491**, 87 (2012).
[72] S. Sevinçli, N. Henkel, C. Ates, and T. Pohl, Nonlocal Nonlinear Optics in Cold Rydberg Gases, Phys. Rev. Lett. **107**, 153001 (2011).
[73] P. Schauss, M. Cheneau, M. Endres, T. Fukuhara, S. Hild, A. Omran, T. Pohl, C. Gross, S. Kuhr, and I. Bloch, Observation of spatially ordered structures in a two-dimensional Rydberg gas, Nature (London) **491**, 87 (2012).
[74] J. Zeiher, J. Y. Choi, A. Rubio-Abadal, T. Pohl, R. Van Bijnen, I. Bloch, and C. Gross, Coherent Many-Body Spin Dynamics in a Long-Range Interacting Ising Chain, Phys. Rev. X **7**, 041063 (2017).